

An Orbital Angular Momentum Feed for 34-Meter Beam Waveguide Antennas

Daniel Hoppe,^{*} Charles Naudet,[†] Julian Breidenthal,[‡] and Gabor Lanyi[†]

ABSTRACT. — Orbital angular momentum (OAM) is a property of electromagnetic waves that can be visualized as a “spiral wavefront” in which surfaces of constant phase are helical surfaces, and the wave’s Poynting vector spirals about a central axis. Traditional applications of Deep Space Network (DSN) antennas use more-or-less planar wavefronts with zero OAM, but this is not the only propagating wave solution to Maxwell’s equations: Other solutions are possible that have non-zero OAM. We designed a special reflective phase plate for insertion to the feed system of DSN 34-m beam-waveguide antennas, that enables both transmission and reception of radio-frequency waves with $m = 1$ OAM. The use of OAM could enable new communication, radar, and science applications for the DSN.

I. Introduction

Electromagnetic waves are a mature field of study, used heavily in the Deep Space Network (DSN) for communication, radar, and science. Traditionally, at radio frequencies, the intensity, coherence, delay, Doppler, and polarization are used to provide a wide range of useful applications. Recently, however, an additional characteristic, the orbital angular momentum (OAM) of electromagnetic waves, has been created and used in the laboratory at visible and radio wavelengths. Waves with OAM have helical instead of plane wavefronts, potentially enabling them to provide rich information about wave sources in reception, and about wave targets in transmission [1]. Radiated energy containing OAM can be used to advantage in radar imaging and other applications [2]. The use of OAM could also enable new communication and science applications.

The theoretical properties of OAM and equations for computing the OAM of a given electromagnetic field are discussed in detail in Barnett [3]. Radio waves with non-zero OAM have been successfully generated or received in different ways, by using uniform circular phased-shifted arrays [2], spiral phase plates (SPP) [4], spiral reflectors [5], and particular modes of horn antennas [6]. The DSN is well positioned to study OAM radar at X-band (~7.2 GHz for spacecraft uplink; ~8.45 GHz for spacecraft downlink; or ~8.56 GHz

^{*} Communications Ground Systems Section.

[†] Deep Space Tracking Systems Section.

[‡] Communication Architectures and Research Section.

for planetary radar), possessing large-diameter (34-meter) beam-waveguide antennas with powerful transmitters, sensitive receivers, and a convenient physical structure that permits changes to antenna feeds at relatively low cost.

We report here a design of feed components, specifically OAM mode 1 and mode 2 SPP feeds for X-band (3.5 cm wavelength), to enable the DSN's 34-meter beam-waveguide research antenna (DSS-13) to explore OAM applications for reception and transmission.

II. Objectives

Our initial objective was to design a non-zero OAM feed for a DSN 34-meter beam-waveguide X-band transmitter. During the course of the study, we found that it was possible to create a non-zero OAM feed for either transmit or receive, by adjusting the assumed frequency incident on the plate.

III. Approach

We designed an OAM feed for the DSS-13 research and development (R&D) 34-meter beam-waveguide antenna at Goldstone, for its 80 KW X-band transmitter. In the first phase of our study, we evaluated tradeoffs between the known methods of generating radio transmissions with OAM, and selected a reflective plate approach because such a device was inexpensive to construct and could be added to the existing antenna with minimal disruption. In the next phase, we determined the feasible range of OAM modes with the selected approach. We also integrated the selected design with the existing antenna beam optics at DSS-13. From this, we derived the expected OAM-mode far-field phase profiles and intensity patterns.

In the simplest form, an OAM beam contains one ($m = 1$) or more ($m > 1$) phase wraps in the azimuthal direction. Self-consistency of phase within the phase wrap also demands that OAM beams have an on-axis null. It is possible to generate an OAM beam through either reflection or transmission of a non-OAM beam through a properly designed electromagnetic structure. An example of a reflective structure is discussed in Tamburini et al. (2012) [5], while a transmissive lens-like structure is covered in Niemiec et al. [4].

In the DSN application, we would like to both transmit and receive OAM beams, with the transmit power as high as 100s of kW CW at frequencies of 7.2 and 8.45 GHz. For this high-power application, the use of dielectrics is problematic, and simple reflective structures are preferable to transmissive ones. Therefore, we chose a simple reflective spiral-cut metal reflector for the DSN application, as depicted in Figure 1. For the spiral-cut reflector, the depth of the reflector, d , is proportional to the azimuthal angle, ϕ , the wavelength, λ , the order of the OAM, m , and the cosine of the angle of incidence on the reflector, θ , that is,

$$d = \frac{m\lambda}{2} * \phi * \cos(\theta) \quad (1)$$

It should be noted that a singularity exists at the center of the reflector, where all values of the azimuthal angle exist for a single point. In practice, a region of small radius about the

reflector center must be excluded. If it is small compared to the wavelength of operation, the exclusion of this region would have minimal impact on overall performance.

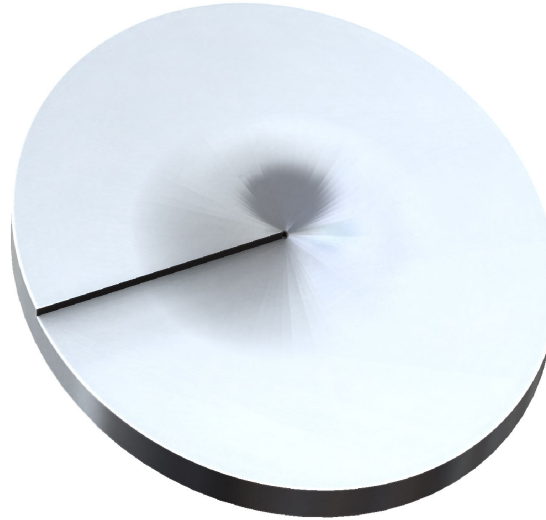


Figure 1. $M = 1$ OAM reflector.

The performance of the OAM reflector was evaluated using physical optics and the commercial software package General Responsibility Assignment Software Patterns (GRASP) [7]. Figure 2 shows the simple GRASP model including a corrugated feed horn and OAM reflector. The reflector was represented as a tabular surface. The model includes a near field plane for evaluation of the near field reflected off the OAM plate in addition to the far field of the composite horn-reflector system. Reflectors for 7.2 and 8.45 GHz, operating in both linear polarization (LP) and circular polarization (CP) were investigated during the course of this work.

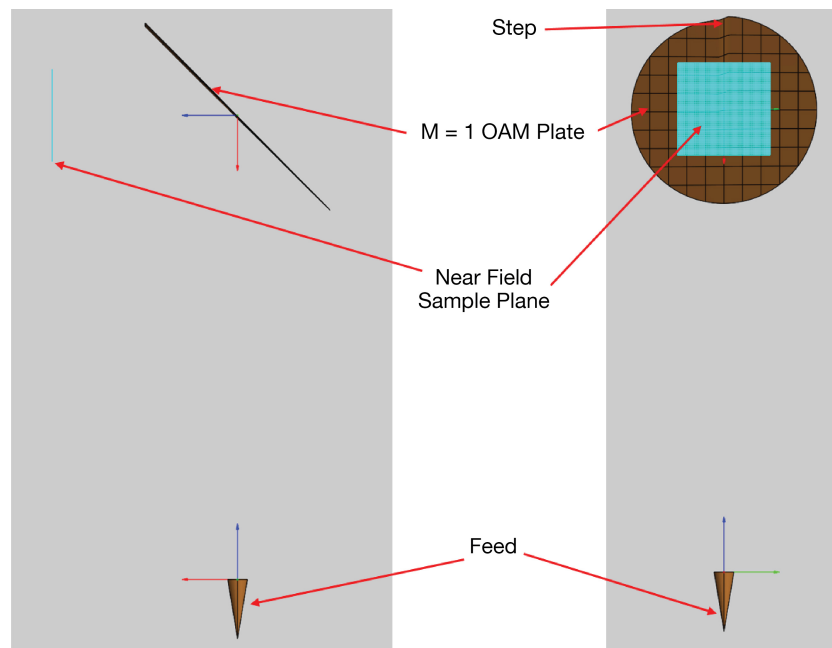


Figure 2. GRASP model of feed and plate.

IV. Results

First, we show the performance of an $m=1$ OAM reflector operating at 7.2 GHz with LP. The angle of incidence is 45 degrees. Contour plots of the far field pattern of the feed-reflector combination are shown in Figure 3. For these plots, the x-axis is $u = \sin(\theta) \cos(\phi)$, and the y-axis is $v = \sin(\theta) \sin(\phi)$. The amplitude pattern on the left shows the expected on-axis null. The phase pattern on the right has a spiral pattern, where the phase ranges from 0 to 360 degrees as the azimuthal angle, ϕ , is traversed.

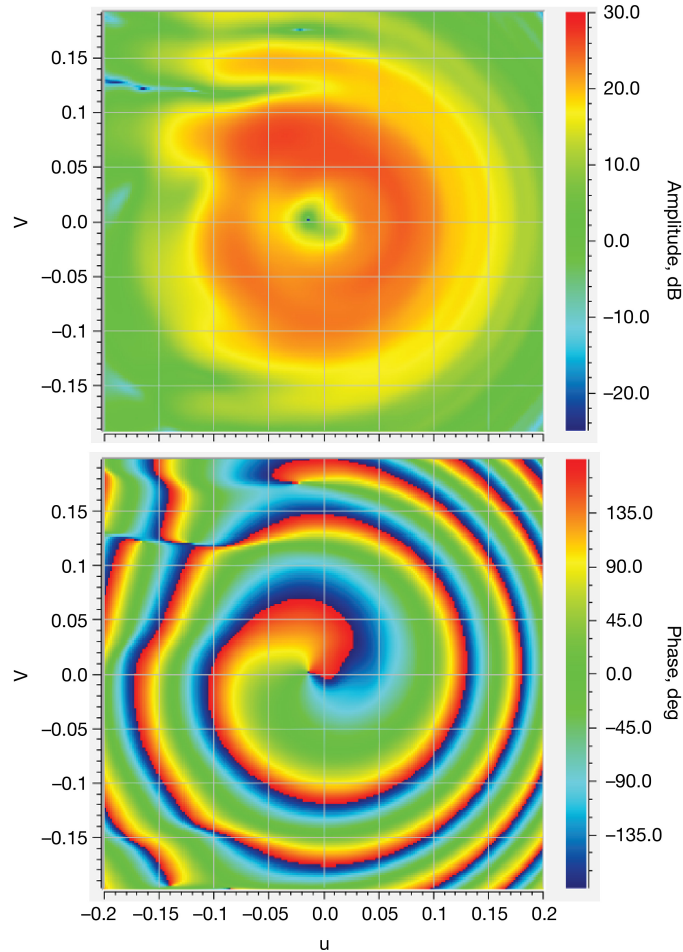


Figure 3. Contour plot of far field feed patterns, $m = 1$ reflector, 7.2 GHz, LP.

Figure 4 shows amplitude cuts through the beam for the co-polarized and cross-polarized components. The cross-polarized fields are approximately 30 dB below the co-polarized peak. A small shift in the null of pattern from $q = 0$ is noted, as well as some asymmetry in the overall pattern. Diffraction effects from the abrupt depth change in the reflector are responsible for both of these phenomena.

After the expected performance of the OAM reflector was confirmed using the free-reflector model, a more complete simulation including the entire 34-meter beam-waveguide antenna was completed. As shown in Figure 5, this GRASP model includes the feed, the OAM reflector, re-imaging ellipsoid, 4-mirror beam-waveguide system, and the shaped primary and secondary surfaces.

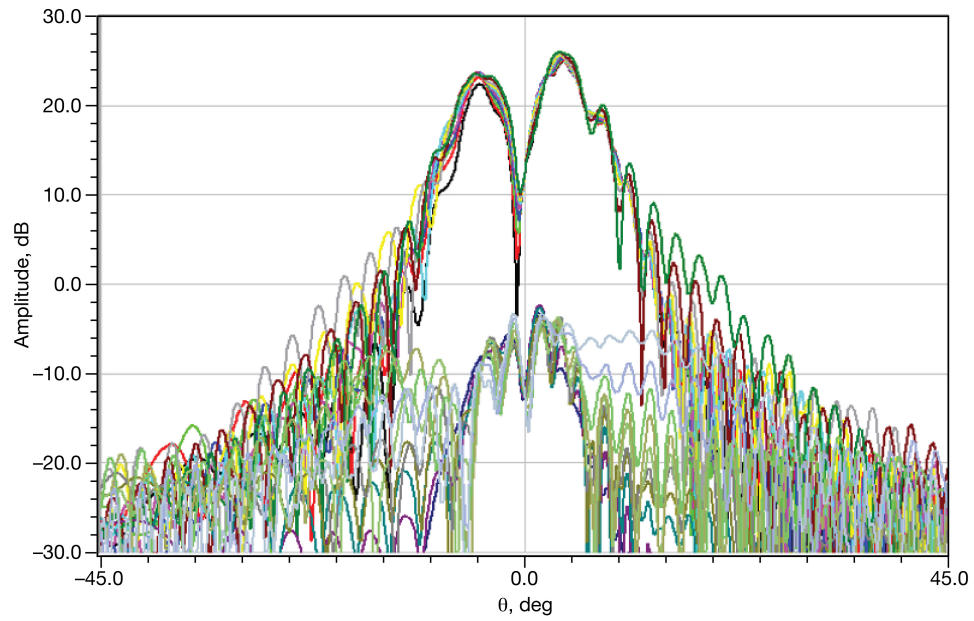


Figure 4. Far field feed pattern cuts, $m = 1$ reflector, 7.2 GHz, LP.

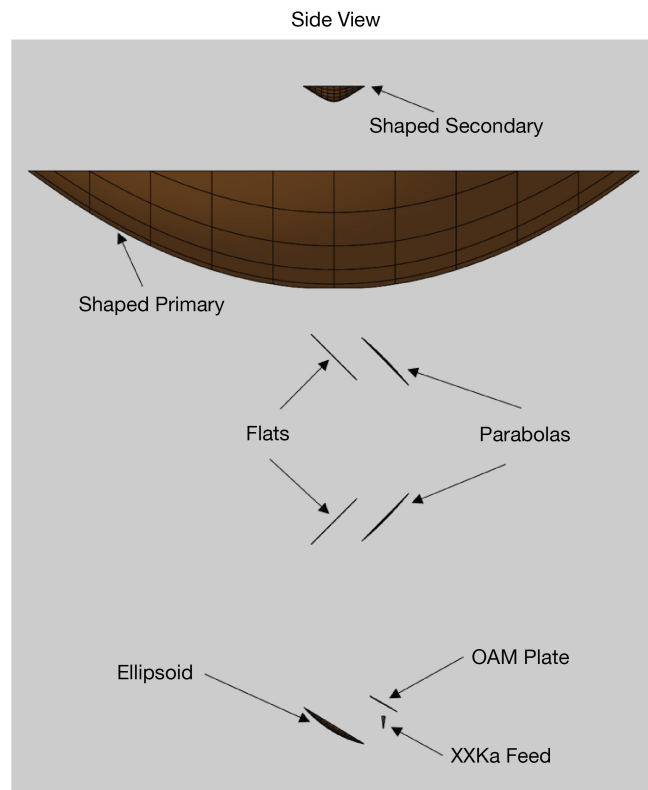


Figure 5. GRASP model of OAM reflector and feed in a 34-m beam-waveguide antenna.

Next, we will show the performance for an 8.45 GHz, $m = 1$, CP system. For this configuration, the angle of incidence on the OAM reflector is 30 degrees. Of interest in this simulation are the amplitude and phase characteristics of the nominal ($m = 0$) and the OAM ($m = 1$) response of the antenna in the far field.

Figures 6 and 7 show contour plots and pattern cuts for the antenna with a flat OAM reflector. This configuration generates the nominal ($m = 0$) mode in the far field. In these patterns, we see the typical Airy pattern for the uniform amplitude and phase illumination of the 34-meter primary. A circularly symmetric phase and amplitude pattern with a 17 dB first side lobe is generated. The computed directivity resulting from the shaped surfaces is 69.25 dB, very near the maximum available from the 34-meter aperture, as expected.

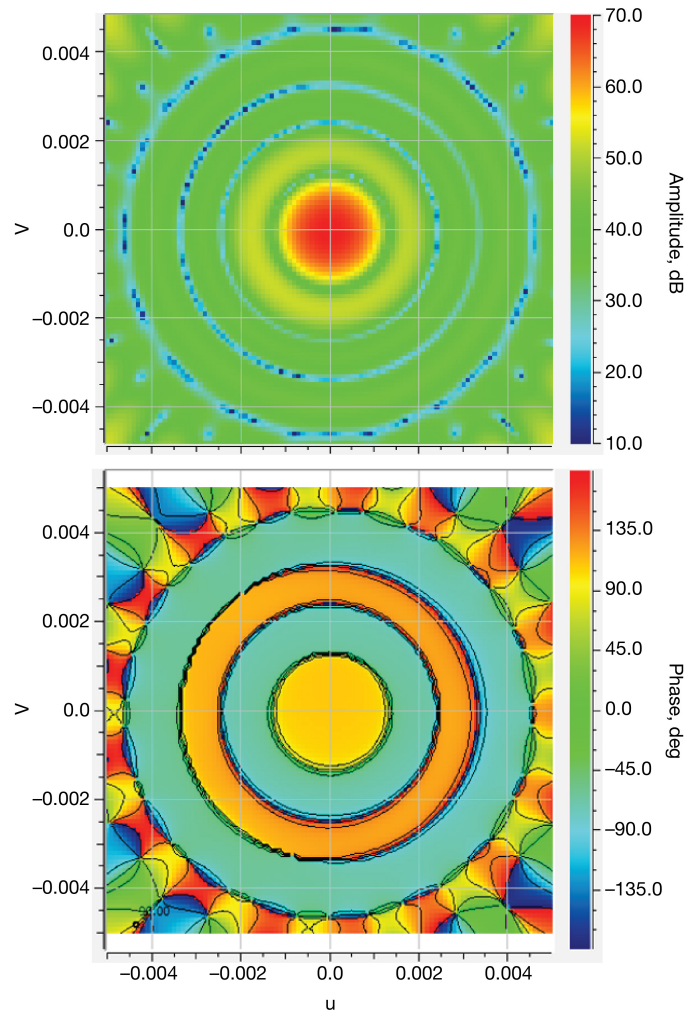


Figure 6. Contour plot of far field antenna pattern, $m = 0$ reflector, 8.45 GHz, CP.

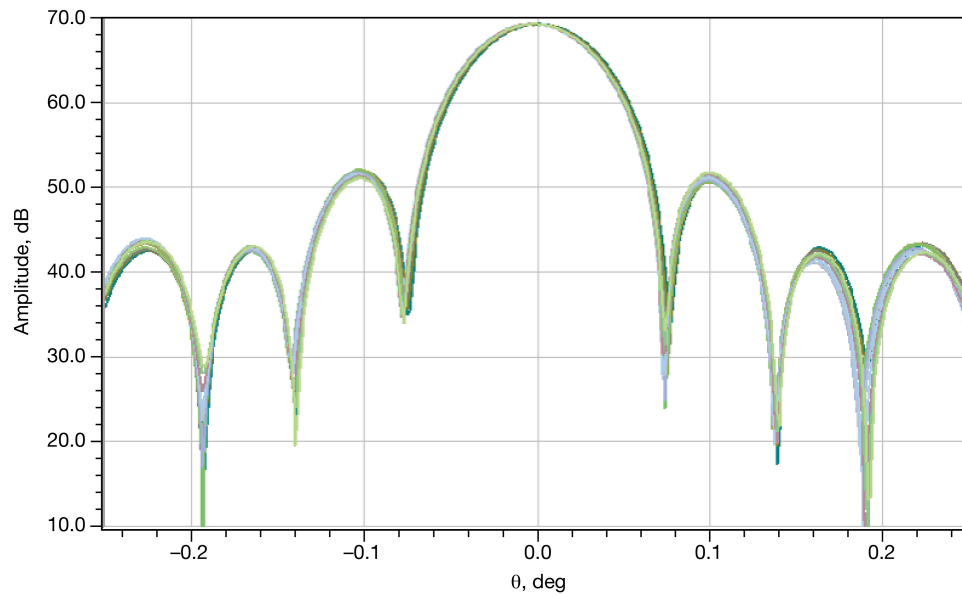


Figure 7. Far field feed pattern cuts, $m = 0$ reflector, 8.45 GHz, CP.

Figures 8 and 9 show contour plots and pattern cuts for the antenna with the $m = 1$ OAM reflector. In these patterns, we see the expected on-axis null and 360-degree phase wrap versus azimuth angle of the 34-meter primary. Once again, diffraction effects are responsible for the observed asymmetry in the beam. The computed directivity for this beam is approximately 63 dB, slightly more than 6 dB below the beam peak for nominal, $m = 1$, operation. In this case, a lateral feed offset relative to the OAM reflector's center of approximately 1 inch in the GRASP model was included to compensate for the slight beam-pointing error in the far field, putting the null very nearly on axis.

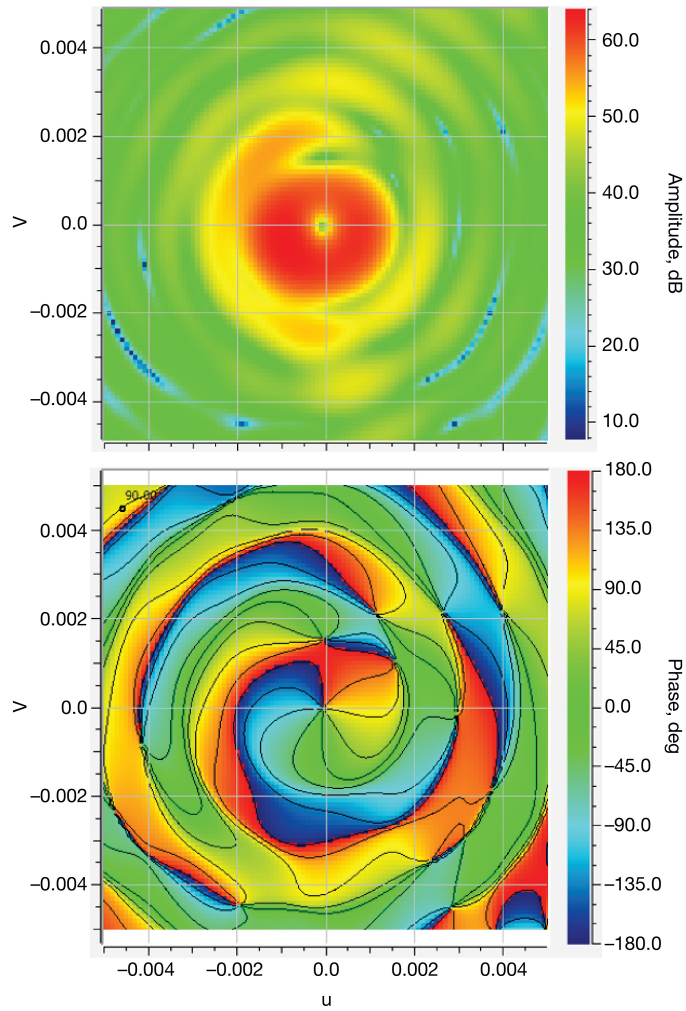


Figure 8. Contour plot of far field antenna pattern, $m = 1$ reflector, 8.45 GHz, CP.

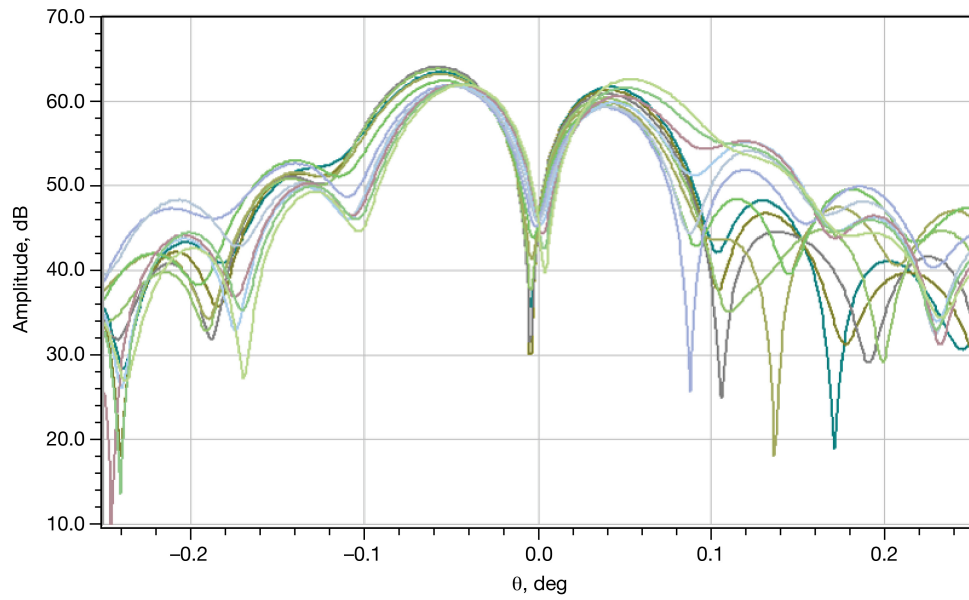


Figure 9. Far field antenna pattern cuts, $m = 1$ reflector, 8.45 GHz, CP.

V. Potential Enhancements

Although this work has shown that OAM beams of reasonable quality can be generated from the DSN antennas using even a simple spiral-cut metal reflector, there are many other approaches for OAM generation and possible improvements. For example, a stepped/segmented OAM reflector such as that depicted in Figure 10 would open the possibility of using a single reflector for multiple frequencies and m-orders, by mechanical actuation of the individual segments. The effect of the discretization on the overall far field pattern can easily be studied with the existing physical optics models. More complicated mixed-m beams can also be generated with OAM reflectors such as the one depicted in Figure 11. Here, the inner portion of the reflector would generate an $m = 0$ beam, while the outer portion would generate an $m = 1$ beam. Applications for such a configuration and performance can also be explored in future work.

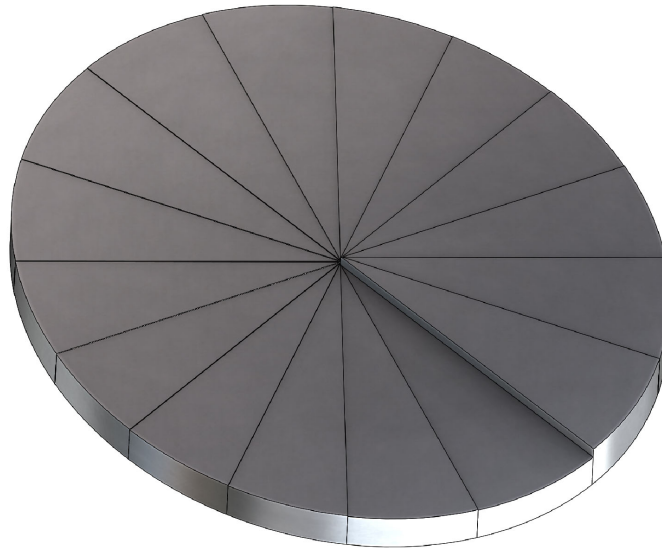


Figure 10. $M = 1$ stepped/segmented reflector.

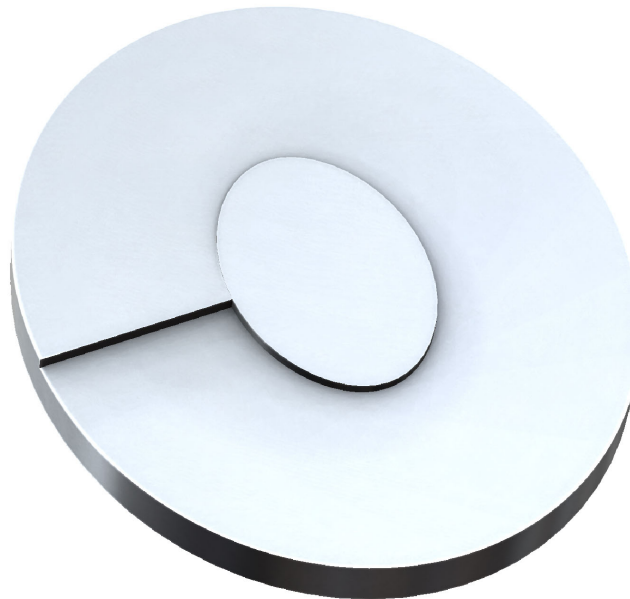


Figure 11. Composite $m = 0/m = 1$ reflector.

VI. Potential Applications

Although studied in depth at optical wavelengths since the early 1990s, the feasibility of generating OAM at radio was not shown until 2007 by Thidé et al. [8]. Most OAM radio studies discuss interesting uses of OAM-based communication, but recently, Liu et al. [2] claimed that OAM-based radar target imaging has the ability to extract azimuthal target information without relative target-illuminator movement. This could yield a breakthrough in the imaging of geostationary satellites, which is an unsolved problem for the Department of Defense's Global Surveillance Program.

Harwit (2003) [9] urged the search for astrophysical OAM sources, and suggested that highly energetic sources such as pulsars would produce OAM from scattering off inhomogeneities in the surrounding environment. Pulsars emit a highly focused "lighthouse" type of beam with a rotation period from milliseconds to seconds, often surrounded by a nebula. The pulsar in the Crab Nebula in particular sweeps around ~30 times a second and has a pulse width less than ~2% of a period, allowing examination of OAM as a function of pulsar rotation. Tamburini et al. (2011) [10] showed that OAM may result from rotating black holes. Sjöholm and Palmer (2007) [11] showed that radio OAM can be a sensitive detector of turbulence in the propagation medium. However, to date, no search for astrophysical OAM sources has been conducted; any detection would open up a new area of study and be of fundamental importance. We believe our proposed observations from DSS-13, with its existing data recorders and processing software proven capable of pulsar detection, offer the best opportunity for the first OAM detection from an astrophysical source. OAM transmission could also be an advantage for some DSN applications in communication and radar.

References

- [1] M. Lin, Y. Gao, P. Liu, J. Liu, "Super-resolution orbital angular momentum based radar targets detection," *Electronics Letters*, vol. 52, no. 13, pp. 1168–1170, 2016.
- [2] K. Liu, Y. Cheng, Z. Yang, H. Wang, Y. Qin, and X. Li, "Orbital-Angular-Momentum-Based Electromagnetic Vortex Imaging," *IEEE Antennas and Wireless Propagation Letters*, vol. 14, pp. 711–714, 2015.
- [3] S. M. Barnett, "Optical Angular-Momentum Flux," *Journal of Optics B: Quantum and Semiclassical Optics*, 4, S7, 2002.
- [4] R. Niemiec, C. Brousseau, K. Mahdjoubi, O. Emile, and A. Menard, "Characterization of an OAM at-Plate Antenna in the Millimeter Frequency Band," *IEEE Antennas and Wireless Propagation Letters*, vol. 13, pp. 1011–1014, 2014.
- [5] F. Tamburini, E. Mari, A. Sponselli, B. Thidé, A. Bianchini, and F. Romanato, "Encoding Many Channels on the Same Frequency Through Radio Vorticity: First Experimental Test," *New Journal of Physics*, vol. 14, 2012.
- [6] Y. H. Choung, K. R. Goudey, L. G. Bryans, "Theory and Design of a Ku-Band TE₂₁-Mode Coupler," *IEEE Transactions on Microwave Theory and Techniques*, vol. 30, no. 11, November 1982. DOI: 10.1109/TMTT.1982.1131335.

- [7] <http://www.ticra.com/software/grasp/>
- [8] B. Thidé, H. Then, J. Sjöholm, K. Palmer, J. Bergman, T. D. Carozzi, Ya. N. Istomin, N. H. Ibragimov, and R. Khamitova, "Utilization of Photon Orbital Angular Momentum in the Low-Frequency Radio Domain," *Physical Review Letters*, vol. 99, no. 8, Article ID 087701, 2007.
- [9] M. Harwit, "Photon Orbital Angular Momentum in Astrophysics," *Astrophysical Journal*, vol. 597, pp 1266–1270, 2003.
- [10] F. Tamburini, B. Thidé, G. Molina-Terriza, G. Anzolin, "Twisting of Light Around Rotating Black Holes," *Nature*, vol. 7, pp. 195–197, 2011.
- [11] J. Sjöholm and K. Palmer, Diploma Thesis, Uppsala University, 2007.